



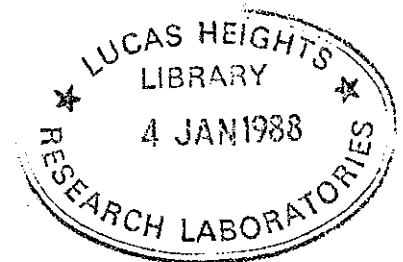
**AUSTRALIAN ATOMIC ENERGY COMMISSION
RESEARCH ESTABLISHMENT**

LUCAS HEIGHTS RESEARCH LABORATORIES

REFERENCE COPY
DO NOT REMOVE FROM LIBRARY

NEUTRON MOISTURE PROBES: THE MINIMUM ERROR ATTAINABLE

by



D. J. WILSON

APRIL 1987

ISBN 0 642 59870 3

AUSTRALIAN ATOMIC ENERGY COMMISSION
RESEARCH ESTABLISHMENT

LUCAS HEIGHTS RESEARCH LABORATORIES

NEUTRON MOISTURE PROBES: THE MINIMUM ERROR ATTAINABLE

by

D. J. WILSON

ABSTRACT

The effect of the soil parameters dry density, mass absorption and mass scattering coefficients on the neutron flux at the detector of a neutron moisture probe has been described previously by a set of polynomial equations. The partial derivatives of these equations have been used to determine the deviation introduced into the water density calculation by a one per cent inaccuracy in each of the parameters. Accuracy of measurement of the soil parameters is discussed and applied to a typical soil at various water densities.

The accuracy to which soil parameters can be measured is examined and found to be approximately $\pm 2\%$ for the dry soil density, $\pm 1\%$ for the mass absorption coefficient and $\pm 2\%$ for the mass scattering coefficient. Using these data, together with a statistical accuracy of $\pm 1\%$ in the probe count rate, the minimum error achievable for the water density varies between $\pm 3.5\%$ at a water density of 0.06 g cm^{-3} and $\pm 1.55\%$ at a water density of 0.41 g cm^{-3} .

National Library of Australia card number and ISBN 0 642 59870 3

The following descriptors have been selected from the INIS Thesaurus to describe the subject content of this report for information retrieval purposes. For further details please refer to IAEA-INIS-12 (INIS: Manual for Indexing) and IAEA-INIS-13 (INIS: Thesaurus) published in Vienna by the International Atomic Energy Agency.

CROSS SECTIONS; ERRORS; MULTIGROUP THEORY; MOISTURE GAGES; NEUTRON FLUX;
NEUTRONS; SOILS; WATER

EDITORIAL NOTE

From 27 April 1987, the Australian Atomic Energy Commission (AAEC) is replaced by Australian Nuclear Science and Technology Organisation (ANSTO). Serial numbers for reports with an issue date after April 1987 have the prefix ANSTO with no change of the symbol (E, M, S or C) or numbering sequence.

CONTENTS

1. INTRODUCTION		1
2. ERRORS DUE TO THE FITTED CURVES		1
3. ERRORS IN THE THERMAL NEUTRON CROSS SECTIONS		2
4. DRY SOIL DENSITY AND ITS ERRORS		3
5. THE ERRORS INTRODUCED INTO THE WATER DENSITY MEASUREMENT BY THE ERRORS IN THE SOIL PARAMETERS		3
5.1 Error in the Water Density Introduced by a 1% Error in Dry Soil Density		3
5.2 Error in the Water Density Introduced by a 1% Error in the Mass Absorption Coefficient		4
5.3 Error in the Water Density Introduced by a 1% Error in the Mass Scattering Coefficient		4
6. OVERALL ACCURACY LIMITS		4
7. COMMENTS		4
8. REFERENCES		5
<hr/>		
Table 1	Derivation of the mass absorption coefficient of Parafield Clay from the chemical analysis of Greacen and Schrale [1976]	7
Table 2	Derivation of the mass scattering coefficient of Parafield Clay from the chemical analysis of Greacen and Schrale [1976]	8
Table 3	Comparison of soil mass absorption coefficients	9
Table 4	Calibration curve for Parafield clay The effect of different mass absorption coefficients	9
Table 5	Per cent error in soil moisture ω due to a +1 per cent error in a soil parameter	10
Table 6	The errors introduced by the most accurate soil parameters	14
Figure 1	The error distribution for calculated water densities using the empirical curves.	15
Figure 2	The percentage error in water density due to +1% error in the dry soil density and the water density. $S_a = 6.305 \times 10^{-3} \text{ cm}^2 \text{ g}^{-1}$; $S_s = 0.12 \text{ cm}^2 \text{ g}^{-1}$	15-16
Figure 3	The percentage error in water density due to +1% error in the mass absorption coefficient and the water density. $S_a = 6.305 \times 10^{-3} \text{ cm}^2 \text{ g}^{-1}$; $S_s = 0.12 \text{ cm}^2 \text{ g}^{-1}$	17-18
Figure 4	The percentage error in water density due to +1% error in the mass scattering coefficient and the water density. $S_a = 6.305 \times 10^{-3} \text{ cm}^2 \text{ g}^{-1}$; $S_s = 0.12 \text{ cm}^2 \text{ g}^{-1}$	18-19
Appendix A	The polynomial fits to multigroup calculations and their partial differentials	21

1. INTRODUCTION

A previous report [Ritchie and Wilson 1984] described the effect of the soil parameters density, mass absorption and mass scattering coefficients on the count rate obtained from the detector of a neutron moisture probe inserted in a borehole. A set of empirical equations was developed which enabled the probe count rate to be interpreted as a soil moisture density over a wide range of soil types and water densities. These equations may be expressed as

$$R(\rho, S_a, S_s, \omega) = \phi_0(\rho, S_a, S_s) \omega^{m(\rho, S_a, S_s)} \quad (1)$$

where R is the response (e.g. count rate), ϕ_0 and m are constants derived by solving in sequence the equations listed in the left hand column of **appendix A**, ρ is the dry soil density (g cm^{-3}) and ω the water density (g cm^{-3}) i.e. the weight of water in each cm^3 of soil. S_a and S_s are the mass absorption and mass scattering coefficients of the soil and are defined respectively as Σ_a/ρ and Σ_s/ρ where Σ_a and Σ_s are respectively the macroscopic absorption and scattering cross sections of the soil.

These empirical curves were fitted by the method of least squares and therefore introduce a fitting error. By differentiating these curves (right hand column of **appendix A**) the errors caused by inaccuracies in the soil parameters can be determined. All of these errors, together with the counting statistics, are summed to determine the error in the water density.

2. ERRORS DUE TO THE FITTED CURVES

Initially, the thermal neutron flux at a moisture probe detector, arising from the fast flux emitted by its source, was calculated using a multigroup, two-dimensional diffusion code, for a range of soil parameters and water densities. These series of points were fitted to empirical curves using the least squares fitting code SUPERFIT [Clancy 1977]. The coefficients of these curves are functions of the soil parameters also found using SUPERFIT. By solving **equations 1-37** of **appendix A**, coefficients are derived in a sequence which eventually results in the correct version of **equation 1** above which relates water density to count rate (R) for the particular soil parameters in use.

This procedure is conveniently processed by a simple computer code. The difference between the calculated water density and the water density used in the original multigroup calculation is the error introduced at that point by inaccuracies in the curve-fitting.

Although it would be possible to achieve a closer fit to the multigroup results by using more complex fitting curves, the precision of the soil parameters does not justify this and the fit was considered to be sufficiently close when the predicted moisture content was nowhere greater than five per cent different from the original calculated points. With this restriction, the variation in the errors cannot have a normal distribution as there will be no tails to the curve. However, a plot of the distribution (**figure 1**) suggests that the distribution of the errors is as close to normal as would be obtained from a set of experiments.

The precision constant, h, determined by the two methods of Sokolnikoff and Sokolnikoff [1941] are

$$h = \frac{1}{|\bar{x}| \sqrt{\pi}} = 0.422 \quad ,$$

$$h = \frac{1}{\sqrt{\bar{x}^2} \sqrt{2}} = 0.415 \quad .$$

As these values are so similar it may be assumed that the mean error on the fits will have similar properties to a standard deviation and therefore can be added in quadrature to the errors described later.

It can be shown [*ibid*] that

$$hE = 0.4769 \quad ,$$

where E is the probable error. Therefore the standard deviation, σ , is given by

$$\sigma = \frac{0.4769}{0.6745h} \quad ,$$

$$= 1.7\% \quad \text{for this data set.}$$

3. ERRORS IN THE THERMAL NEUTRON CROSS SECTIONS

The neutron absorption and scattering cross sections can be obtained by chemical analysis of soil and the published microscopic (atomic) cross sections [Mughabghab *et al.* 1981].

The main problem with this approach is to ensure that the sample analysed is representative of the volume of soil seen by the neutrons and that all of the elements contributing significantly to the macroscopic cross section are included in the analysis. About half of the elemental material is oxygen occurring as oxides and this, apart from hydrogen, is the main contributor to the scattering component. The errors arising in this method stem from the analysis which determines the elemental fractions in the soil; the ensured inclusion of all the significant elements (*i.e.* those contributing to the total cross section); the accuracy to which the microscopic absorption cross sections are known (typically one to five per cent); and the degree to which the small soil sample analysed is representative of the volume seen by the neutron probe. In particular, the fraction of the most significant element boron must be suspect at these low levels. It is interesting to note the improvement in the accuracy of these cross sections over the years 1973-1981. **Tables 1** and **2** show the mass absorption and mass scattering coefficients obtained in this way for the Parafield clay soil analysis of Greacen and Schrale [1976], in which the errors are determined from the published accuracies in the cross sections and by assuming the error in the fractions to be \pm one digit in the last figure which is considerably smaller than the true error.

Another technique is to introduce a sample of soil into the centre of a critical nuclear reactor. The subsequent power transient is a function of the absorption and scattering cross sections and can be analysed using inverse kinetic techniques [*e.g.* Harries 1978] or by measuring the asymptotic doubling or halving time of the transient [McCulloch and Wall 1976]. These are not absolute methods and the reactor transient analysis must be compared to that obtained when using standards of known cross section.

The errors introduced with this technique are systematic, due to inaccuracies in the standards used, and statistical, due to instabilities in the reactor resulting mainly from ambient temperature variations. In the present state of ANSTO's 10 kW research reactor Moata, the error in the measured soil mass absorption coefficient is about $\pm 0.4 \times 10^{-3} \text{ cm}^2 \text{ g}^{-1}$, but if temperature variations could be compensated for, this figure could be reduced to about $\pm 0.1 \times 10^{-3} \text{ cm}^2 \text{ g}^{-1}$. The size of the sample used in the measurement is 200 g and is a reasonable fraction of the volume seen by the probe.

A comparison of results from these analyses is given in **table 3**. Although the chemical analysis technique appears to be more accurate, it must be remembered that the error quoted does not include a realistic error for the elemental fraction determined by chemical analysis. Also the lower values for three of the chemical analysis results suggest that some significant elements have been missed. This, of course, cannot happen in the reactor analysis but the reactor neutron spectrum must be considered when assessing the absorption coefficient.

The effect of the absorption coefficient can be demonstrated by using the data for Parafield clay and making best fits to the measurements of Greacen and Schrale [1976]. The calibration curves are developed using the mass absorption and mass scattering coefficients obtained from chemical analysis or by reactor measurement. After subtracting the effect of bound hydrogen in each case ($1.471 \times 10^{-3} \text{ cm}^2 \text{ g}^{-1}$), the values are

$$\begin{aligned} S_a (1) \text{ (chemical)} &= 8.337 \times 10^{-3} \text{ cm}^2 \text{ g}^{-1} \quad , \\ S_a (2) \text{ (reactor)} &= 10.43 \times 10^{-3} \text{ cm}^2 \text{ g}^{-1} \quad . \end{aligned}$$

ω_1 and ω_2 are the water densities calculated for various count rates at these two mass absorption coefficients and are given in **table 4**. Both sets of figures are normalised to the experimental points at a water density around 0.285 g cm^{-3} . This illustrates the errors which occur if the calibration curve is normalised at a single point, say in a drum of the moist soil, and the wrong value for S_a is used. In this particular case the maximum error is only about three per cent.

If the calibration point relies on normalisation in a different soil for which $S_a = 8.337 \times 10^{-3} \text{ cm}^2 \text{ g}^{-1}$ and the measurements are made in a soil for which $S_a = 10.45 \times 10^{-3} \text{ cm}^2 \text{ g}^{-1}$ but is thought to be $8.337 \times 10^{-3} \text{ cm}^2 \text{ g}^{-1}$, the results will be as for ω_3 , the errors being up to 12 per cent. It can be seen from this that missing a significant soil constituent can introduce substantial errors unless a single point calibration is made in each soil.

4. DRY SOIL DENSITY AND ITS ERRORS

As the thermal neutron flux at the detector is a function of the dry soil density, this must be measured and its error estimated. The error may be due to variations in the soil structure or to shortcomings in the measuring device.

The density may be obtained by sampling the soil in the neighbourhood of the bore, or even from the core of the bore hole. A convenient method is to use a gamma density probe as this can be used to scan the hole or move from hole to hole. The shape of the calibration curve of a gamma backscattering density probe depends upon the geometry of the probe and the electron density of the soil [Christensen 1973a, 1973b]. As the geometry factors such as the source/detector separation, the length of the gamma shield and its diameter relative to the detector diameter are fixed for a particular probe, the main source of error is probably the change in electron density in the soil, particularly when moisture is present. The correction for the presence of water requires an iterative procedure between the neutron probe analysis, which requires the dry soil density, and the gamma probe analysis which requires the water content.

Rawls and Brooks [1975] measured samples of dried soils from a field survey using a gamma probe, but found that the bulk densities obtained resulted in some unrealistic water densities (up to 117 per cent saturated). Subsequent assessment suggested that the dry soil density was in error by about 25 per cent and correcting this reduced the water density to 76 per cent saturation. This illustrates the necessity for accurate density measurements.

Ciftcioglu and Taylor [1971], using a gamma backscatter density gauge with differential mode counting, stated that this technique is capable of an accuracy of $\pm 2\%$.

5. THE ERRORS INTRODUCED INTO THE WATER DENSITY MEASUREMENT BY THE ERRORS IN THE SOIL PARAMETERS

Equation 1 can be used to estimate the uncertainty in the water density, ω , arising from uncertainties in the response, R , which arise as a result of uncertainties in the dry soil density, ρ , and the mass absorption and scattering coefficients, S_a and S_s at particular values of these parameters.

The following conditions are sought [Wilson and Ritchie 1986]:

$$\left. \frac{\partial R}{\partial S_a} \right|_{\rho, S_s} = 0 ; \quad \left. \frac{\partial R}{\partial \rho} \right|_{S_a, S_s} = 0 ; \quad \left. \frac{\partial R}{\partial S_s} \right|_{\rho, S_a} = 0 , \quad (2)$$

which, from equation 1, yields

$$\left. \frac{\Delta \omega}{\omega} \right|_{\rho, S_a} = - \left[\frac{1}{\phi_o m} \cdot \frac{\partial \phi_o}{\partial S_s} + \frac{n \omega}{m} \cdot \frac{\partial m}{\partial S_s} \right] \Delta S_s , \quad (3)$$

$$\left. \frac{\Delta \omega}{\omega} \right|_{S_a, S_s} = - \left[\frac{1}{\phi_o m} \cdot \frac{\partial \phi_o}{\partial \rho} + \frac{n \omega}{m} \cdot \frac{\partial m}{\partial \rho} \right] \Delta \rho , \quad (4)$$

$$\left. \frac{\Delta \omega}{\omega} \right|_{S_s, \rho} = - \left[\frac{1}{\phi_o m} \cdot \frac{\partial \phi_o}{\partial S_a} + \frac{n \omega}{m} \cdot \frac{\partial m}{\partial S_a} \right] \Delta S_a . \quad (5)$$

The partial derivatives are obtained from the original fitted curves and are given in appendix A.

Equations to calculate these errors are incorporated into a computer program and the error due to each parameter is printed out separately, together with the addition in quadrature. This allows the adequacy of the data to be considered. Typical introduced errors are presented in figures 2a-c, 3a-c, 4a-c. A more complete set, together with tables of errors, is given in table 5. The correctness of the differentials has been checked by comparing the calculated error with the differences produced by changing each parameter separately by one per cent.

5.1 Error in the Water Density Introduced by a 1% Error in Dry Soil Density

If the density is overestimated by one per cent, the water density will be underestimated by about the same amount, as shown in figures 2a-c. Figure 2a shows the effect at different densities but at fixed mass

absorption and scattering coefficients. The maximum effect occurs at a density of about 1.8 g cm^{-3} . Figure 2b shows that errors in the density are greatest for soils with a low mass absorption coefficient and figure 2c shows the error to have most effect for soils with high mass scattering coefficient. The figures show that for all soil types the effect is greatest at low water densities.

5.2 Error in the Water Density Introduced by a 1% Error in the Mass Absorption Coefficient

Figures 3a-c are typical results; figure 3a shows the error in the water density introduced by a one per cent error in the absorption coefficient at various dry soil densities but with fixed absorption and scattering coefficients. The error is greatest at high dry soil densities. Figure 3b shows the effect at various soil absorption coefficients. The effect changes with the water density and soil parameters in a complex manner, peaking at a mass absorption coefficient value which is a function of all the other soil parameters. Figure 3c is rather misleading as it suggests the change in the water density introduced by a one per cent change in the mass absorption coefficient is the same over a range of mass scattering coefficients. An examination of table 5 shows that this is true only at the chosen values of S_a ($6.305 \times 10^{-3} \text{ cm}^2 \text{ g}^{-1}$) and ρ (1.33 g cm^{-3}). For other values of these parameters the error due to an error in the mass absorption coefficient is more dependent on the magnitude of the mass scattering coefficient and their curves equivalent to those of figure 3c would be more divergent.

5.3 Error in the Water Density Introduced by a 1% Error in the Mass Scattering Coefficient

Figures 4a-c illustrate the fact that at low water densities an error in the mass scattering coefficient can introduce errors in the water density up to three times those due to a similar percentage error in S_a or ρ . The mass scattering coefficient must be determined accurately, otherwise a single point normalisation in the soil with a known water density is necessary. Apart from bound hydrogen, over 95 per cent of the mass scattering coefficient is likely to be due to the elements Si, Al, Fe, O and C.

6. OVERALL ACCURACY LIMITS

Clearly, the accuracy of the derived water density will depend on the magnitude and uncertainties of the parameters describing the soil and the absolute value of the water density.

At first glance it appears that chemical analysis and microscopic cross sections will result in an extremely accurate value for S_a and S_s . This is not necessarily the case, for the soil may contain unexpected elements. It is quite common to find 50-100 parts per million of boron which is not only difficult to measure accurately at these levels, but may contribute half the total mass absorption coefficient. Chemical analysis is usually carried out for the elements requested, and a highly absorbing trace element may be missed.

Reactor analyses of cross sections have the advantage that the overall cross section of the sample is measured regardless of constituents. There is however a fairly constant lower limit of detectable signal due to noise and the lower values of mass absorption coefficient can only be measured to $\sim \pm 0.4 \times 10^{-3} \text{ cm}^2 \text{ g}^{-1}$. This lower limit is expected to be reduced to $\sim 0.1 \times 10^{-3} \text{ cm}^2 \text{ g}^{-1}$ which represents about $\pm 1\%$.

Mass scattering coefficients can probably be measured to $\pm 2\%$ by chemical methods as the presence of trace elements will not affect the value and with care the density can be determined to $\pm 2\%$.

Using the above values of the inaccuracies in the soil parameters, say

$$\rho = 1.5 \pm 0.03 \text{ g cm}^{-3} ,$$

$$S_a = (10.0 \pm 0.1) \times 10^{-3} \text{ cm}^2 \text{ g}^{-1} ,$$

$$S_s = 0.12 \pm 0.0024 \text{ cm}^2 \text{ g}^{-1} ,$$

and including a statistical error of $\pm 1\%$ in the count rate, the standard deviation in the water density varies between $\pm 3.5\%$ and $\pm 1.55\%$ according to the water density. Full details of the deviation introduced by each of the above inaccuracies and the sum in quadrature are given in table 7. Note how the error in the mass scattering coefficient dominates.

7. COMMENTS

These results represent what is probably the highest accuracy obtainable using current methods, for the measurement of water density in a drum of homogeneous soil of sufficient size to be considered infinitely large to neutrons from the probe source. No effect of the bore hole lining material or the possible inaccuracies or variations in the equivalence of water in the gamma density measurement has been considered.

Having produced a calibration curve such as that from **table 7**, measurements in the same homogeneous soil elsewhere would be subject to the added extra count rate and density deviation (in quadrature). Measurements in a different homogeneous soil with approximately the same parameters arising from different analysis but using the same normalisation, would have minimum standard deviation approximately $\sqrt{2} \times$ those of **table 5**.

8. REFERENCES

- Christensen, E.R. [1973a] - Use of the gamma density gauge in combination with the neutron moisture probe. *Proc. Symp. Isotopes and Radiation Techniques in Soil Physics and Irrigation Studies*, Vienna, 1-8 October. IAEA-SM-176/1.
- Christensen, E.R. [1973b] - Monte Carlo calculations for the subsurface gamma density gauge. *Nucl. Eng. Des.*, 24:431-439.
- Ciftcioglu, O., Taylor, D. [1971] - A gamma backscatter density gauge with differential mode counting. *Nucl. Instrum. Methods*, 94:53-59.
- Clancy, B.E. [1977] - SUPERFIT - an interactive program for function evaluation and least squares fitting. AAEC/E408.
- Greacen, E.L., Schrale, G. [1976] - The effect of bulk density on neutron meter calibration. *Aust. J. Soil Res.*, 14:159-169.
- Harries, J.R. [1978] - Inverse kinetics reactivity measurements on the materials testing reactor HIFAR. AAEC/E456.
- McCulloch, D.B., Wall, T. [1976] - A method of measuring the neutron absorption cross section of soil samples for calibration of the neutron moisture meter. *Nucl. Instrum. Methods*, 137:577-581.
- Mughabghab, S.F., Garber, D.I. [1973] - Neutron cross sections, Volume 1. BNL325. (3rd Edition).
- Mughabghab, S.F., Divadeenam, M., Holden, N.E. [1981] - Neutron Cross Sections. Vol. 1, part A. Academic Press, N.Y.
- Rawls, W.J., Brooks, R.H. [1975] - Gamma probe dry bulk densities. *Soil Sci.*, 120:68-70.
- Ritchie, A.I.M., Wilson, D.J. [1984] - Investigation of the response of a neutron moisture meter using a multigroup, two-dimensional diffusion code. AAEC/E579.
- Sokolnikoff, I.S., Sokolnikoff, E.S. [1941] - Higher Mathematics for Engineers and Physicists. McGraw Hill, New York and London, 2nd edition.
- Wilson, D.J., Ritchie, A.I.M. [1986] - Neutron moisture meters: the dependence of their response on soil parameters. *Aust. J. Soil Res.*, 24:11-23.

NOTES

TABLE 1
DERIVATION OF THE MASS ABSORPTION COEFFICIENT OF PARAFIELD CLAY
FROM THE CHEMICAL ANALYSIS OF GREACEN AND SCHRALE [1976]

Analysis		Mass Absorption Coefficient S_a ($\text{cm}^2 \text{g}^{-1}$)							
Element	Weight Fraction	σ_a (1) barns	Partial S_a (1) $\times 10^6$	% Error*	Abs. Error $\times 10^6$	σ_a (2) barns	Partial S_a (2) $\times 10^6$	% Error*	Abs. Error $\times 10^6$
Si	0.2688	0.17 \pm 0.02	980	11.76	115	0.171 \pm 0.003	986	1.75	17
Al	0.09630	0.235 \pm 0.005	505	2.13	11	0.231 \pm 0.003	497	1.30	6
Fe	0.05960	2.55 \pm 0.05	1639	1.96	32	2.56 \pm 0.03	1646	1.17	19
Ti	0.00530	6.1 \pm 0.2	407	3.28	13	6.09 \pm 0.13	406	2.14	9
Mn	0.00037	13.3 \pm 0.1	54	2.81	2	13.3 \pm 0.2	54	3.09	2
Ca	0.00350	0.43 \pm 0.02	23	4.66	1	0.43 \pm 0.02	23	4.66	1
Mg	0.01060	0.063 \pm 0.005	17	7.94	1	0.063 \pm 0.003	17	4.76	1
K	0.02260	2.1 \pm 0.1	731	4.76	35	2.1 \pm 0.1	731	4.76	35
Na	0.0050	0.527 \pm 0.010	69	2.76	2	0.530 \pm 0.0007	69	2.00	1
[†] H	0.00740	0.332 \pm 0.0021	1468	0.62	9	0.3326 \pm 0.0007	1471	0.25	4
O	0.514	27 $\times 10^{-5}$	5	3.71	0	(28.0 \pm 2.0) $\times 10^{-5}$	4	10.53	0
P	0.00044	0.18 \pm 0.02	2	11.34	0	0.172 \pm 0.006	1	4.16	0
N	0.00040	1.90 \pm 0.03	33	2.96	1	1.9 \pm 0.03	33	2.96	1
C	0.00400	0.0034 \pm 0.0002	1	5.89	0	0.0035 \pm 0.0001	1	2.87	0
B	0.000090	759 \pm 2	3806	1.14	43	767 \pm 8	3846	1.52	59
Cl	0.00004	33.2 \pm 0.5	23	25.05	6	33.1 \pm 0.3	23	25.02	6

S_a (1) = 0.009763 \pm 0.000133** = (1.36%); S_a (2) = 0.009808 \pm 0.000074** (0.75%).

Microscopic absorption cross section σ_a (1) from BNL 325 [1973]; σ_a (2) from Mughabghab *et al.* [1981].

σ_a for oxygen includes the (n, α) cross section.

* Assumes an error of ± 1 in the last figure of the weight fraction together with the error in σ_a .

** Addition in quadrature.

[†] H is a special case because of the way its scattering cross section behaves when the hydrogen is bound. It is better to consider hydrogen bound in soil as part of the water, calculate total water and remove bound hydrogen after. Without the bound hydrogen, S_a (1) becomes 0.008295 \pm 0.000133 (1.60%) and S_a (2) = 0.008337 \pm 0.000074 (1.60%).

TABLE 2
DERIVATION OF THE MASS SCATTERING COEFFICIENT OF PARAFIELD CLAY
FROM THE CHEMICAL ANALYSIS OF GREACEN AND SCHRALE [1976]

Analysis		Mass Scattering Coefficient S_s ($\text{cm}^2 \text{g}^{-1}$)							
Element	Weight Fraction	σ_s (1) barns	Partial S_s (1) $\times 10^6$	% Error*	Abs. Error $\times 10^6$	σ_s (2) barns	Partial S_s (2) $\times 10^6$	% Error*	Abs. Error $\times 10^6$
Si	0.2688	2.2 \pm 0.2	12682	9.09	1153	2.0437 \pm 0.0017	11781	0.09	11
Al	0.09630	1.40 \pm 0.03	3010	2.14	65	1.4134 \pm 0.0010	3039	0.07	2
Fe	0.05960	11.39 \pm 0.04	7321	0.35	26	11.35 \pm 0.03	7295	0.26	19
Ti	0.00503	4.2 \pm 0.2	266	4.77	13	4.09 \pm 0.03	259	0.76	2
Mn	0.00037	1.9 \pm 0.1	8	5.92	0	2.2 \pm 0.2	9	9.48	1
Ca	0.00350	3.0 \pm 0.3	158	10.00	16	2.93 \pm 0.04	154	1.39	2
Mg	0.01060	3.41 \pm 0.10	896	2.93	26	3.4140 \pm 0.0024	897	0.12	1
K	0.02260	2.1 \pm 0.1	737	4.76	35	2.04 \pm 0.10	710	4.90	35
Na	0.0050	3.1 \pm 0.2	406	6.75	27	3.025 \pm 0.020	396	2.11	8
H†	0.00740	20.4 \pm 0.1	90211	0.51	370	20.491 \pm 0.014	90624	0.15	137
O	0.514	3.76 \pm 0.02	72755	0.57	412	3.761 \pm 0.006	72774	0.25	183
P	0.00044	3.4 \pm 0.30	29	9.11	3	3.134 \pm 0.010	27	2.30	1
N	0.00040	10.6 \pm 0.5	182	5.34	10	10.03 \pm 0.08	173	2.62	5
C	0.00400	4.71 \pm 0.04	945	0.89	8	4.740 \pm 0.005	951	0.27	3
B	0.000090	3.7 \pm 0.2	19	5.52	1	4.27 \pm 0.07	21	2.00	0
Cl	0.00004	15.0 \pm 0.2	10	25.04	3	15.8 \pm 0.2	11	25.03	3

S_s (1) = 0.189635 \pm 0.001282** (0.67%); S_s (2) = 0.18911 \pm 0.000233** (0.12%).

Microscopic scattering cross section σ_s (1) from BNL 325 [1973]; σ_s (2) from Mughabghab *et al.* [1981].

* Assumes an error of ± 1 in the last figure of the weight fraction together with the error in σ_s .

** Addition in quadrature.

† H is a special case because of the way its scattering cross section behaves when the hydrogen is bound. It is better to consider hydrogen bound in soil as part of the water, calculate total water and remove bound hydrogen after. Without the bound hydrogen, the scattering cross sections are S_s (1) = 0.099424 \pm 0.001228 (\pm 1.23%); S_s (2) = 0.098487 \pm 0.000188 (\pm 0.19%).

TABLE 3
COMPARISON OF SOIL MASS ABSORPTION COEFFICIENTS

Soil Type	Mass Absorption Coefficients ($\text{cm}^2 \text{g}^{-1} \times 10^{-3}$)		
	Chemical	Chemical	Reactor
	Analysis	Analysis	Analysis
	1	2	3
Parafield loam	8.91	9.09±0.07	8.84±0.38
Long Flat clay	8.98	9.09±0.06	9.08±0.44
Parafield clay	9.66	9.81±0.07	11.90±0.43
Narayan sand	4.43	5.04±0.09	4.99±0.32
Konetta soil	4.34	4.35±0.10	6.03±0.33
Sturt River aluvium	6.21	6.34±0.06	8.86±0.47

1. Using the chemical analysis of Greacen and Schrale [1976] (see for example table 2 for Parafield clay) and using the microscopic absorption cross sections from BNL 325 [1973].
2. As for 1 but using the later cross section evaluations from Mughabghab *et al.* [1981].
3. Measured value using the technique of McCulloch and Wall [1976] independent of chemical analysis.

TABLE 4
CALIBRATION CURVE FOR PARAFIELD CLAY
THE EFFECT OF DIFFERENT MASS ABSORPTION COEFFICIENTS

Count Rate	% Difference		% Difference		
	ω_1	ω_2	$100 (\omega_1 - \omega_2) / \bar{\omega}$	ω_3	$100 (\omega_1 - \omega_3) / \bar{\omega}$
0.05	0.089	0.092	-3.3	0.100	11.6
0.1	0.147	0.150	-2.0	0.162	9.7
0.15	0.197	0.199	-1.0	0.215	8.7
0.2	0.242	0.243	-0.4	0.263	8.3
0.25	0.285	0.285	0.0	0.308	7.8
0.3	0.325	0.324	0.3	0.350	7.4
0.35	0.363	0.360	0.8	0.390	7.2
0.4	0.400	0.396	1.0	0.428	6.8

- ω_1 $S_a = 8.337 \times 10^{-3} \text{ cm}^2 \text{ g}^{-1}$ } Normalised so that the count rate is 0.25
 ω_2 $S_a = 10.43 \times 10^{-3} \text{ cm}^2 \text{ g}^{-1}$ } at a water density of 0.285 g cm^{-3} .
 ω_3 $S_a = 10.43 \times 10^{-3} \text{ cm}^2 \text{ g}^{-1}$ with same normalising factor as ω_1 .

TABLE 5
PER CENT ERROR IN SOIL MOISTURE ω DUE TO A
+ 1 PER CENT ERROR IN A SOIL PARAMETER

$$S_s = 0.10 \text{ cm}^2 \text{ g}^{-1}$$

ω (g cm ⁻³)		0.1					0.2					0.3					0.4				
$S_a \times 10^{-3}$	ρ	$\frac{\Delta\omega}{\Delta\rho}$	$\frac{\Delta\omega}{\Delta S_a}$	$\frac{\Delta\omega}{\Delta S_s}$	$\frac{\Delta\omega}{\Delta\rho}$	$\frac{\Delta\omega}{\Delta S_a}$	$\frac{\Delta\omega}{\Delta S_s}$	$\frac{\Delta\omega}{\Delta\rho}$	$\frac{\Delta\omega}{\Delta S_a}$	$\frac{\Delta\omega}{\Delta S_s}$	$\frac{\Delta\omega}{\Delta\rho}$	$\frac{\Delta\omega}{\Delta S_a}$	$\frac{\Delta\omega}{\Delta S_s}$	$\frac{\Delta\omega}{\Delta\rho}$	$\frac{\Delta\omega}{\Delta S_a}$	$\frac{\Delta\omega}{\Delta S_s}$					
cm ² g ⁻¹	g cm ⁻³																				
1.708	0.5	-0.392	0.101	-0.520	-0.284	0.073	-0.376	-0.220	0.057	-0.291	-0.175	0.045	-0.230								
	1.0	-0.752	0.184	-0.776	-0.551	0.145	-0.575	-0.435	0.122	-0.458	-0.351	0.106	-0.373								
	1.33	-0.910	0.237	-0.965	-0.677	0.194	-0.728	-0.541	0.169	-0.589	-0.445	0.151	-0.491								
	1.667	-0.945	0.289	-1.164	-0.721	0.244	-0.894	-0.590	0.218	-0.736	-0.497	0.199	-0.624								
	2.0	-0.804	0.341	-1.557	-0.643	0.295	-1.060	-0.549	0.268	-0.886	-0.482	0.249	-0.762								
6.305	0.5	-0.232	0.262	-0.464	-0.151	0.189	-0.344	-0.105	0.147	-0.274	-0.072	0.117	-0.224								
	1.0	-0.515	0.409	-0.747	-0.346	0.317	-0.560	-0.244	0.261	-0.447	-0.172	0.222	-0.368								
	1.33	-0.657	0.484	-0.921	-0.443	0.385	-0.695	-0.318	0.327	-0.562	-0.229	0.286	-0.468								
	1.667	-0.678	0.546	-1.083	-0.463	0.445	-0.827	-0.337	0.385	-0.677	-0.247	0.343	-0.570								
	2.0	-0.490	0.601	-1.228	-0.343	0.497	-0.950	-0.257	0.436	-0.787	-0.196	0.393	-0.672								
12.61	0.5	-0.114	0.335	-0.414	-0.053	0.256	-0.305	-0.018	0.209	-0.241	0.008	0.177	-0.196								
	1.00	-0.369	0.477	-0.717	-0.208	0.390	-0.539	-0.114	0.339	-0.435	-0.047	0.304	-0.360								
	1.33	-0.513	0.551	-0.913	-0.300	0.468	-0.701	-0.174	0.420	-0.577	-0.085	0.386	-0.489								
	1.667	-0.520	0.622	-1.119	-0.306	0.544	-0.881	-0.180	0.499	-0.742	-0.091	0.467	-0.643								
	2.0	-0.258	0.701	-1.337	-0.141	0.619	-1.078	-0.072	0.571	-0.925	-0.024	0.537	-0.817								
18.91	0.5	-0.068	0.285	-0.358	-0.009	0.249	-0.239	0.025	0.227	-0.169	0.050	0.211	-0.118								
	1.00	-0.333	0.324	-0.592	-0.156	0.317	-0.420	-0.053	0.313	0.319	0.020	0.311	-0.248								
	1.33	-0.480	0.336	-0.772	-0.242	0.357	-0.576	-0.103	0.370	0.460	-0.004	0.379	-0.379								
	1.667	-0.448	0.361	-1.016	-0.223	0.403	-0.797	-0.091	0.428	-0.669	0.003	0.446	-0.578								
	2.0	-0.061	0.425	-1.337	0.012	0.461	-1.090	0.054	0.481	-0.946	0.084	0.496	-0.843								

TABLE 5 (cont'd)

$$S_a = 0.11 \text{ cm}^2 \text{ g}^{-1}$$

ω (g cm ⁻³)		0.1			0.2			0.3			0.4		
$S_a \times 10^{-3}$	ρ	$\frac{\Delta\omega}{\Delta\rho}$	$\frac{\Delta\omega}{\Delta S_a}$	$\frac{\Delta\omega}{\Delta S_b}$	$\frac{\Delta\omega}{\Delta\rho}$	$\frac{\Delta\omega}{\Delta S_a}$	$\frac{\Delta\omega}{\Delta S_b}$	$\frac{\Delta\omega}{\Delta\rho}$	$\frac{\Delta\omega}{\Delta S_a}$	$\frac{\Delta\omega}{\Delta S_b}$	$\frac{\Delta\omega}{\Delta\rho}$	$\frac{\Delta\omega}{\Delta S_a}$	$\frac{\Delta\omega}{\Delta S_b}$
cm ² g ⁻¹	g cm ⁻³												
1.708	0.5	-0.417	0.105	-0.524	-0.301	0.076	-0.372	-0.234	0.059	-0.282	-0.186	0.047	-0.219
	1.00	-0.804	0.192	-0.815	-0.592	0.153	-0.597	-0.468	0.129	-0.469	-0.380	0.113	-0.378
	1.33	-0.983	0.253	-1.023	-0.736	0.209	-0.763	-0.592	0.184	-0.611	-0.489	0.166	-0.502
	1.67	-1.034	0.316	-1.225	-0.795	0.270	-0.929	-0.655	0.244	-0.755	-0.556	0.225	-0.632
	2.0	-0.898	0.379	-1.396	-0.725	0.333	-1.076	-0.624	0.305	-0.889	-0.552	0.286	-0.755
6.305	0.5	-0.259	0.269	-0.483	-0.171	0.193	-0.345	-0.119	0.149	-0.264	-0.082	0.117	-0.206
	1.00	-0.560	0.414	-0.773	-0.376	0.319	-0.569	-0.268	0.263	-0.450	-0.191	0.223	-0.364
	1.33	-0.708	0.490	-0.971	-0.481	0.389	-0.727	-0.347	0.330	-0.584	-0.252	0.288	-0.482
	1.67	-0.729	0.555	-1.158	-0.501	0.451	-0.881	-0.368	0.391	-0.719	-0.273	0.348	-0.604
	2.0	-0.530	0.612	-1.308	-0.375	0.505	-1.012	-0.284	0.443	-0.839	-0.219	0.399	-0.715
12.61	0.5	-0.142	0.349	-0.443	-0.072	0.268	-0.312	-0.032	0.220	-0.235	-0.003	0.186	-0.181
	1.00	-0.413	0.498	-0.741	-0.239	0.409	-0.548	-0.137	0.357	-0.435	-0.065	0.320	-0.355
	1.33	-0.564	0.576	-0.965	-0.337	0.491	-0.735	-0.203	0.442	-0.600	-0.109	0.406	-0.504
	1.67	-0.573	0.649	-1.200	-0.347	0.568	-0.940	-0.214	0.521	-0.787	-0.120	0.488	-0.679
	2.00	-0.309	0.725	-1.413	-0.183	0.640	-1.136	-0.109	0.591	-0.974	-0.057	0.555	-0.859
18.91	0.5	-0.090	0.311	-0.394	-0.023	0.278	-0.260	-0.016	0.258	-0.181	0.043	0.244	-0.126
	1.00	-0.368	0.389	-0.645	-0.180	0.381	-0.458	-0.069	0.376	-0.348	0.009	0.373	-0.271
	1.33	-0.524	0.425	-0.867	-0.274	0.443	-0.646	-0.128	0.454	-0.517	-0.024	0.461	-0.425
	1.67	-0.508	0.466	-1.135	-0.271	0.504	-0.886	-0.132	0.526	-0.740	-0.033	0.542	-0.636
	2.0	-0.142	0.527	-1.413	-0.057	0.560	-1.136	-0.007	0.579	-0.974	0.029	0.592	-0.877

(continued)

TABLE 5 (cont'd)

$$S_b = 0.12 \text{ cm}^2 \text{ g}^{-1}$$

ω (g cm ⁻³)		0.1			0.2			0.3			0.4		
$S_a \times 10^{-3}$	ρ	$\frac{\Delta\omega}{\Delta\rho}$	$\frac{\Delta\omega}{\Delta S_a}$	$\frac{\Delta\omega}{\Delta S_b}$	$\frac{\Delta\omega}{\Delta\rho}$	$\frac{\Delta\omega}{\Delta S_a}$	$\frac{\Delta\omega}{\Delta S_b}$	$\frac{\Delta\omega}{\Delta\rho}$	$\frac{\Delta\omega}{\Delta S_a}$	$\frac{\Delta\omega}{\Delta S_b}$	$\frac{\Delta\omega}{\Delta\rho}$	$\frac{\Delta\omega}{\Delta S_a}$	$\frac{\Delta\omega}{\Delta S_b}$
cm ² g ⁻¹	g cm ⁻³												
1.708	0.50	-0.442	0.108	-0.492	-0.321	0.078	-0.335	-0.250	0.060	-0.243	-0.200	0.048	-0.178
	1.00	-0.858	0.200	-0.819	-0.635	0.160	-0.585	-0.504	0.136	-0.448	-0.411	0.120	-0.351
	1.33	-1.055	0.267	-1.045	-0.794	0.223	-0.762	-0.641	0.197	-0.597	-0.532	0.178	-0.479
	1.67	-1.115	0.338	-1.250	-0.862	0.264	-0.927	-0.714	0.264	-0.738	-0.609	0.245	-0.604
	2.00	-0.970	0.412	-1.397	-0.789	0.364	-1.053	-0.683	0.335	-0.852	-0.608	0.315	-0.708
6.305	0.50	-0.280	0.272	-0.483	-0.187	0.195	-0.326	-0.132	0.151	-0.235	-0.093	0.119	-0.170
	1.00	-0.604	0.419	-0.773	-0.409	0.323	-0.557	-0.295	0.266	-0.431	-0.214	0.226	-0.341
	1.33	-0.761	0.497	-0.995	-0.521	0.394	-0.737	-0.380	0.334	-0.585	-0.280	0.292	-0.478
	1.67	-0.779	0.563	-1.209	-0.540	0.458	-0.915	-0.400	0.396	-0.742	-0.301	0.353	-0.620
	2.00	-0.557	0.623	-1.366	-0.397	0.513	-1.054	-0.303	0.450	-0.872	-0.237	0.405	-0.742
12.61	0.50	-0.160	0.356	-0.472	-0.086	0.274	-0.320	-0.043	0.226	-0.231	-0.012	0.192	-0.168
	1.00	-0.456	0.513	-0.759	-0.271	0.422	-0.557	-0.163	0.369	-0.438	-0.086	0.331	-0.354
	1.33	-0.617	0.594	-1.019	-0.377	0.507	-0.775	-0.237	0.457	-0.631	-0.137	0.421	-0.530
	1.67	-0.623	0.669	-1.291	-0.386	0.587	-1.012	-0.247	0.539	-0.848	-0.149	0.505	-0.732
	2.00	-0.327	0.747	-1.501	-0.201	0.660	-1.211	-0.127	0.609	-1.041	-0.074	0.573	-0.921
18.91	0.50	-0.102	0.327	-0.453	-0.032	0.293	-0.310	0.009	0.274	-0.226	0.038	0.259	-0.166
	1.00	-0.402	0.430	-0.737	-0.204	0.420	-0.541	-0.088	0.415	-0.425	-0.006	0.411	-0.344
	1.33	-0.571	0.484	-1.024	-0.308	0.501	-0.781	-0.153	0.512	-0.639	-0.044	0.519	-0.537
	1.67	-0.550	0.544	-1.338	-0.302	0.582	-1.058	-0.157	0.604	-0.893	-0.054	0.620	-0.776
	2.00	-0.145	0.623	-1.568	-0.063	0.655	-1.284	-0.015	0.673	-1.117	0.019	0.686	-0.999

TABLE 5 (cont'd)

$$S_s = 0.13 \text{ cm}^2 \text{ g}^{-1}$$

$\omega \text{ (g cm}^{-3}\text{)}$		0.1					0.2					0.3					0.4				
$S_a \times 10^{-3}$	ρ	$\frac{\Delta\omega}{\Delta\rho}$	$\frac{\Delta\omega}{\Delta S_a}$	$\frac{\Delta\omega}{\Delta S_s}$	$\frac{\Delta\omega}{\Delta\rho}$	$\frac{\Delta\omega}{\Delta S_a}$	$\frac{\Delta\omega}{\Delta S_s}$	$\frac{\Delta\omega}{\Delta\rho}$	$\frac{\Delta\omega}{\Delta S_a}$	$\frac{\Delta\omega}{\Delta S_s}$	$\frac{\Delta\omega}{\Delta\rho}$	$\frac{\Delta\omega}{\Delta S_a}$	$\frac{\Delta\omega}{\Delta S_s}$	$\frac{\Delta\omega}{\Delta\rho}$	$\frac{\Delta\omega}{\Delta S_a}$	$\frac{\Delta\omega}{\Delta S_s}$					
$\text{cm}^2 \text{ g}^{-1}$	g cm^{-3}																				
1.708	0.50	-0.469	0.109	-0.519	-0.342	0.079	-0.360	-0.267	0.062	-0.267	-0.214	0.050	-0.201								
	1.00	-0.919	0.208	-0.896	-0.681	0.167	-0.648	-0.542	0.143	-0.502	-0.443	0.126	-0.399								
	1.33	-1.128	0.279	-1.143	-0.851	0.234	-0.838	-0.689	0.207	-0.660	-0.574	0.188	-0.533								
	1.67	-1.181	0.355	-1.345	-0.917	0.307	-0.997	-0.762	0.280	-0.794	-0.651	0.260	-0.649								
	2.00	-1.001	0.434	-1.442	-0.821	0.384	-1.083	-0.715	0.356	-0.873	-0.640	0.335	-0.723								
6.305	0.50	-0.298	0.273	-0.511	-0.201	0.197	-0.335	-0.144	0.153	-0.233	-0.104	0.121	-0.160								
	1.00	-0.652	0.428	-0.808	-0.446	0.329	-0.580	-0.326	0.271	-0.447	-0.240	0.231	-0.353								
	1.33	-0.826	0.507	-1.064	-0.571	0.402	-0.792	-0.421	0.340	-0.632	-0.315	0.297	-0.519								
	1.67	-0.838	0.573	-1.314	-0.587	0.465	-1.003	-0.439	0.402	-0.820	-0.335	0.358	-0.691								
	2.00	-0.569	0.633	-1.474	-0.411	0.522	-1.152	-0.319	0.456	-0.963	-0.253	0.410	-0.829								
12.61	0.50	-0.171	0.360	-0.500	-0.095	0.277	-0.324	-0.050	0.228	-0.221	-0.019	0.194	-0.148								
	1.00	-0.501	0.522	-0.771	-0.306	0.430	-0.560	-0.192	0.376	-0.436	-0.111	0.337	-0.348								
	1.33	-0.683	0.605	-1.075	-0.428	0.517	-0.817	-0.278	0.466	-0.666	-0.172	0.430	-0.558								
	1.67	-0.681	0.682	-1.396	-0.432	0.600	-1.098	-0.287	0.551	-0.922	-0.183	0.517	-0.798								
	2.00	-0.319	0.768	-1.602	-0.201	0.679	-1.301	-0.131	0.627	-1.124	-0.082	0.590	-0.999								
18.91	0.50	-0.110	0.334	-0.489	-0.038	0.295	-0.336	0.004	0.272	-0.246	0.034	0.256	-0.182								
	1.00	-0.448	0.441	-0.798	-0.237	0.431	-0.593	-0.113	0.425	-0.473	-0.026	0.421	-0.387								
	1.33	-0.634	0.505	-1.159	-0.353	0.526	-0.891	-0.188	0.538	-0.734	-0.070	0.546	-0.623								
	1.67	-0.587	0.587	-1.524	-0.328	0.630	-1.208	-0.176	0.655	-1.023	-0.069	0.673	-0.891								
	2.00	-0.074	0.705	-1.690	-0.012	0.738	-1.389	0.024	0.757	-1.213	0.050	0.771	-1.087								

TABLE 6
THE ERRORS INTRODUCED BY THE MOST
ACCURATE SOIL PARAMETERS

Dry density	(ρ)	=	$1.5 \pm 0.03 \text{ g cm}^{-3}$
Mass absorption coefficient	(S_a)	=	$10.0 \pm 0.10 \times 10^{-3} \text{ cm}^2 \text{ g}^{-1}$
Mass scattering coefficient	(S_s)	=	$0.12 \pm 0.0024 \text{ cm}^2 \text{ g}^{-1}$

Count rate : statistical error $\pm 1.0\%$ for all counts

Water Density (g cm^{-3})	Counts	$\pm\%$ Deviation Due to				Total*
		ρ	S_a	S_s		
0.062	0.817	1.727	0.692	2.633	3.326	
0.110	0.817	1.327	0.607	2.199	2.763	
0.153	0.817	1.092	0.557	1.944	2.439	
0.194	0.817	0.924	0.522	1.763	2.214	
0.232	0.817	0.795	0.495	1.623	2.044	
0.270	0.817	0.688	0.472	1.507	1.907	
0.306	0.817	0.599	0.453	1.410	1.794	
0.341	0.817	0.521	0.437	1.326	1.699	
0.376	0.817	0.452	0.422	1.251	1.617	
0.410	0.817	0.390	0.409	1.184	1.546	

* Sum of deviations in quadrature.

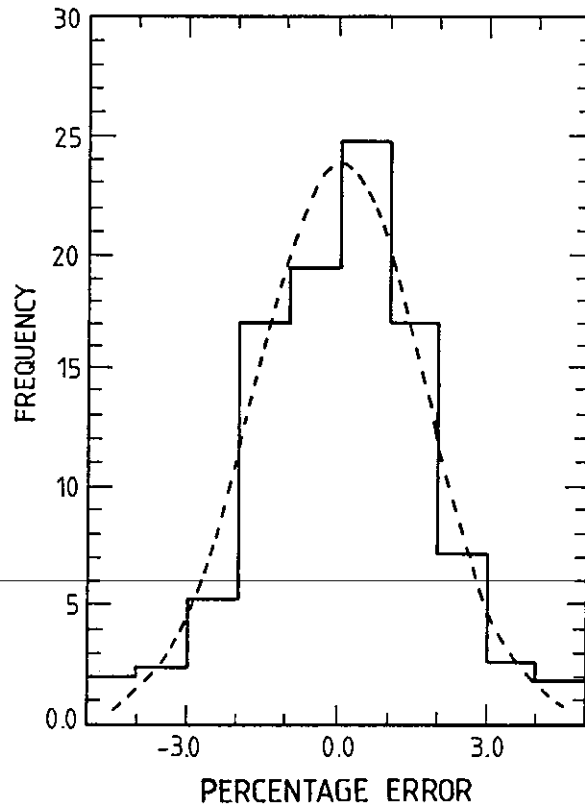


Figure 1 The error distribution for calculated water densities using the empirical curves. The broken line is the fitted normal distribution.

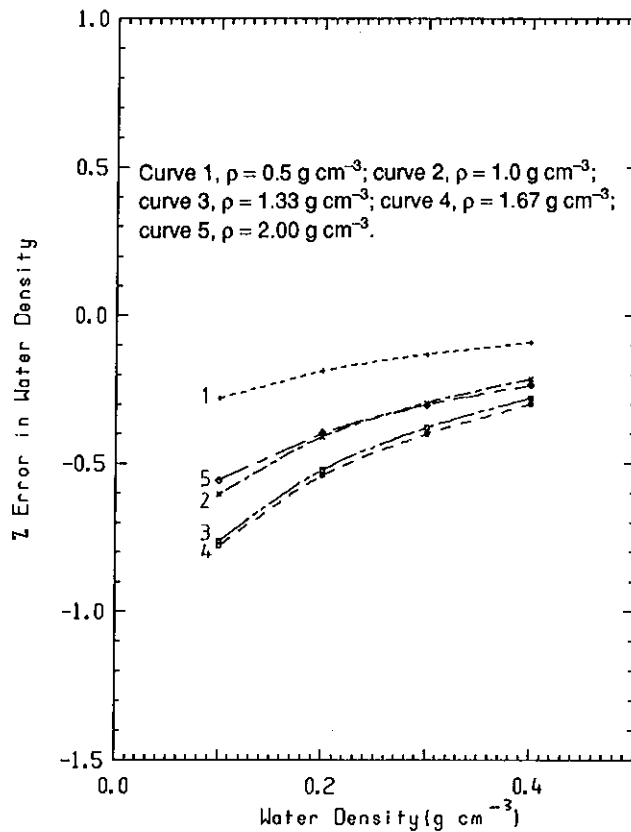


Figure 2a The percentage error in water density due to +1% error in the dry soil density; the effect of the dry soil density and the water density: $S_a = 6.305 \times 10^{-3} \text{ cm}^2 \text{ g}^{-1}$; $S_s = 0.12 \text{ cm}^2 \text{ g}^{-1}$.

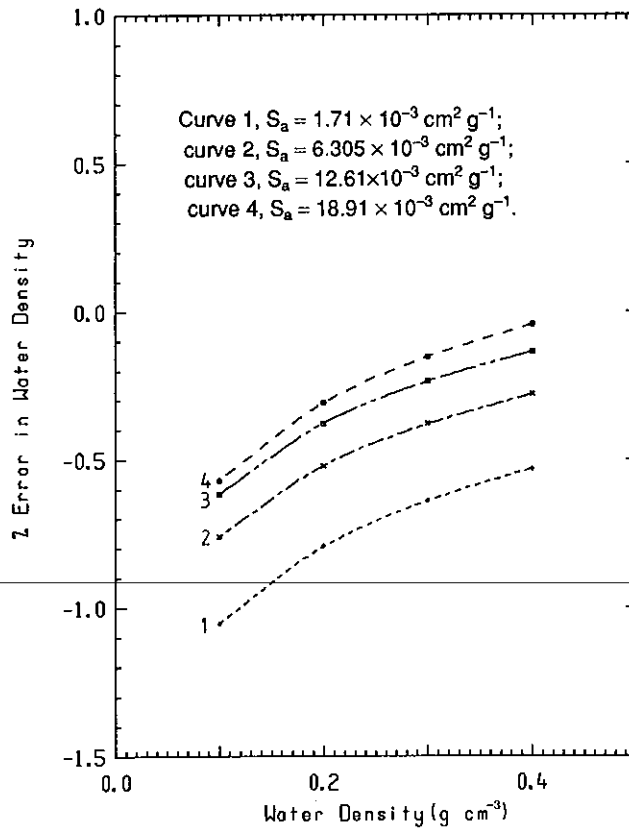


Figure 2b The percentage error in water density due to +1% error in the dry soil density; the effect of the mass absorption coefficient and the water density: $\rho = 1.33 \text{ g cm}^{-3}$, $S_s = 0.12 \text{ cm}^2 \text{ g}^{-1}$.

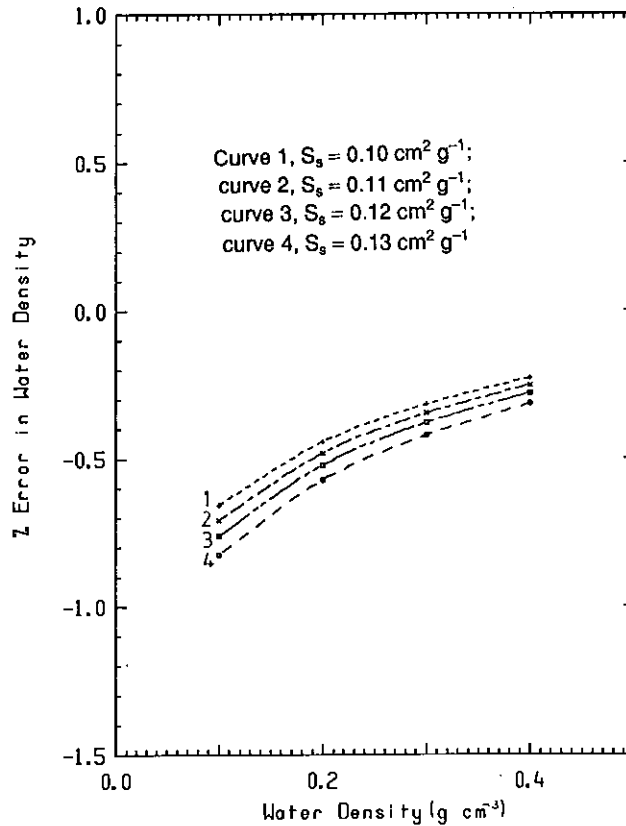


Figure 2c The percentage error in water density due to +1% error in the dry soil density; the effect of the mass scattering coefficient and the water density: $\rho = 1.33 \text{ g cm}^{-3}$, $S_a = 6.305 \times 10^{-3} \text{ cm}^2 \text{ g}^{-1}$.

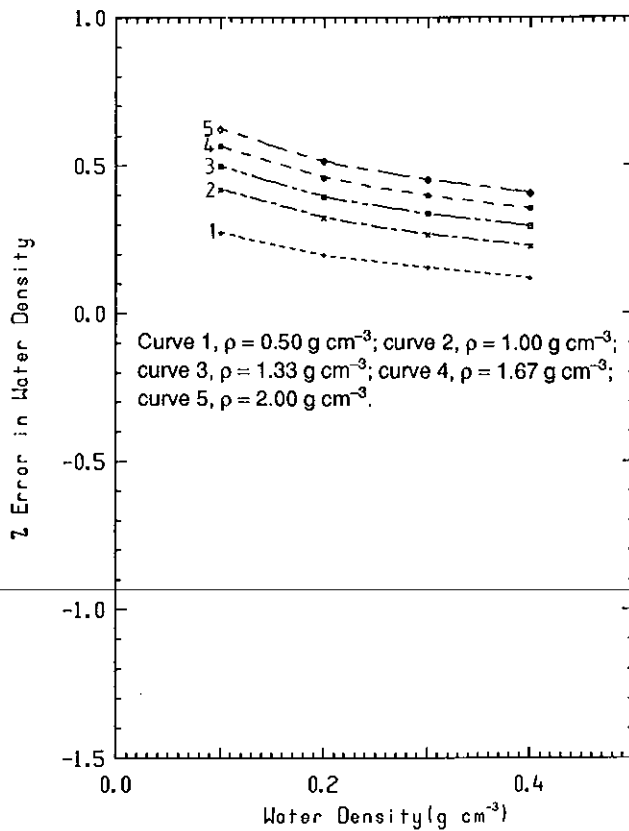


Figure 3a The percentage error in water density due to +1% error in the mass absorption coefficient; the effect of the dry soil density and the water density: $S_a = 6.305 \times 10^{-3} \text{ cm}^2 \text{ g}^{-1}$; $S_s = 0.12 \text{ cm}^2 \text{ g}^{-1}$.

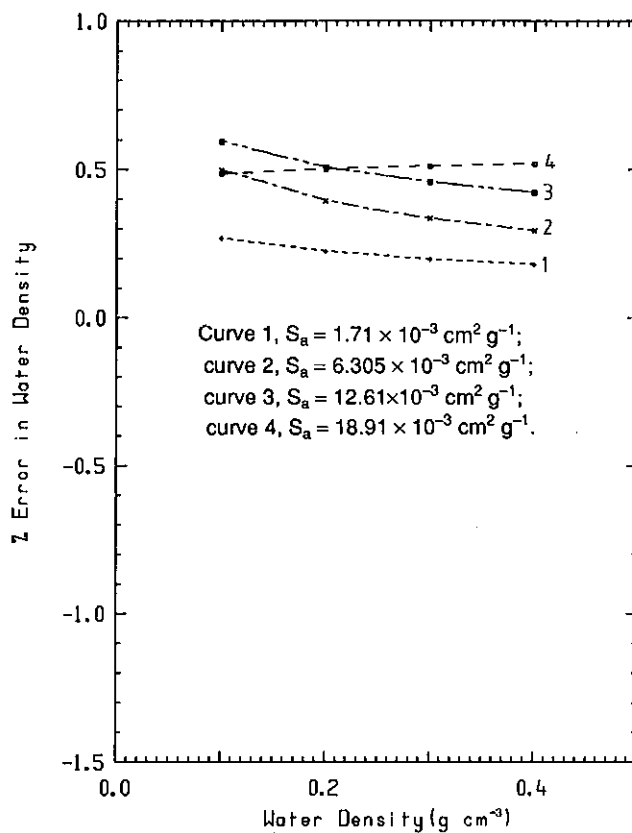


Figure 3b The percentage error in water density due to +1% error in the mass absorption coefficient; the effect of the mass absorption coefficient and the water density: $\rho = 1.33 \text{ g cm}^{-3}$, $S_s = 0.12 \text{ cm}^2 \text{ g}^{-1}$.

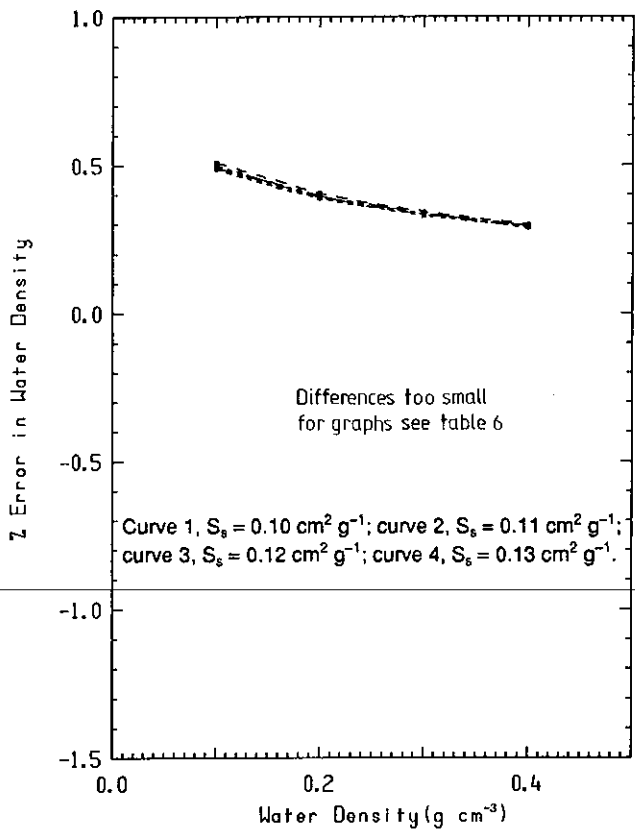


Figure 3c The percentage error in water density due to +1% error in the mass absorption coefficient; the effect of the mass scattering coefficient and the water density: $\rho = 1.33 \text{ g cm}^{-3}$; $S_a = 6.305 \times 10^{-3} \text{ cm}^2 \text{ g}^{-1}$.

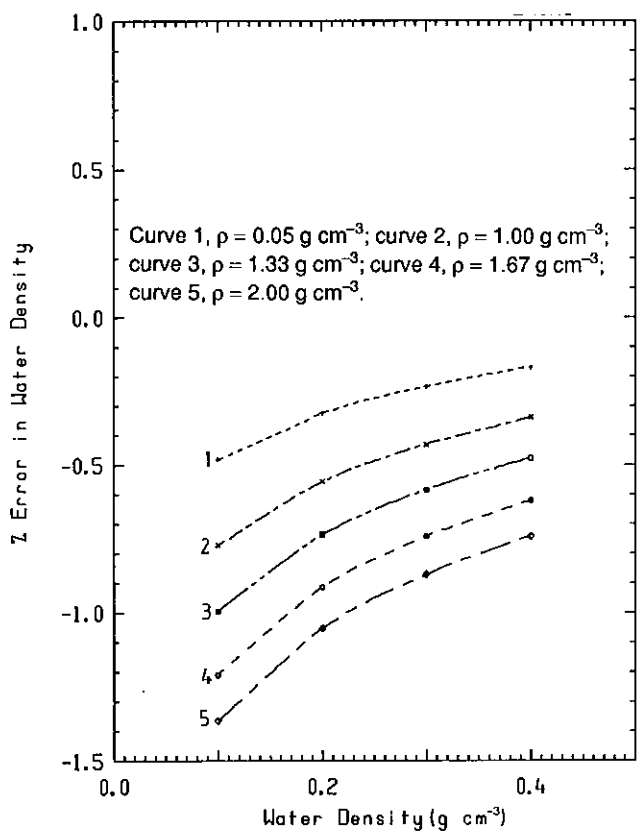


Figure 4a The percentage error in water density due to +1% error in the mass scattering coefficient; the effect of the dry soil density and the water density: $S_a = 6.305 \times 10^{-3} \text{ cm}^2 \text{ g}^{-1}$; $S_s = 0.12 \text{ cm}^2 \text{ g}^{-1}$.

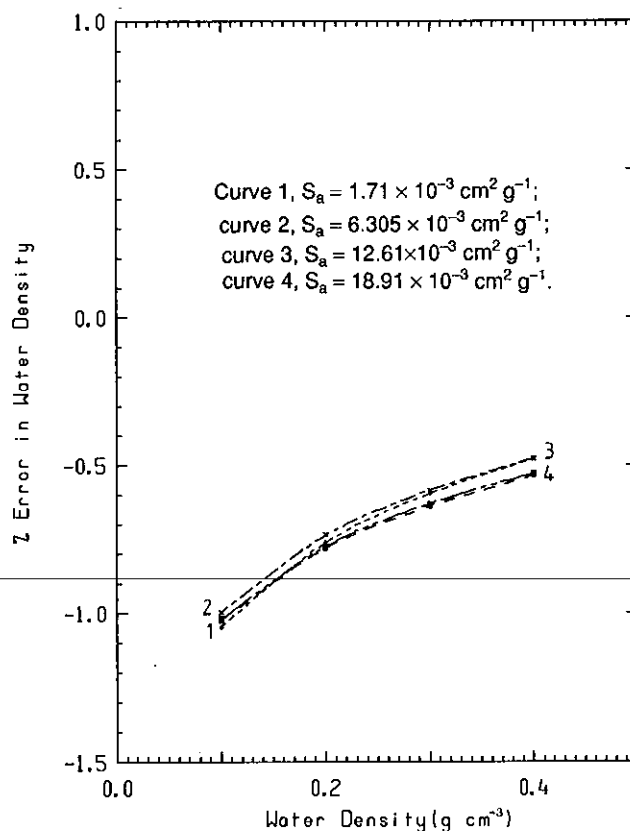


Figure 4b The percentage error in water density due to +1% error in the mass scattering coefficient; the effect of the mass absorption coefficient and the water density: $\rho = 1.33 \text{ g cm}^{-3}$, $S_s = 0.12 \text{ cm}^2 \text{ g}^{-1}$.

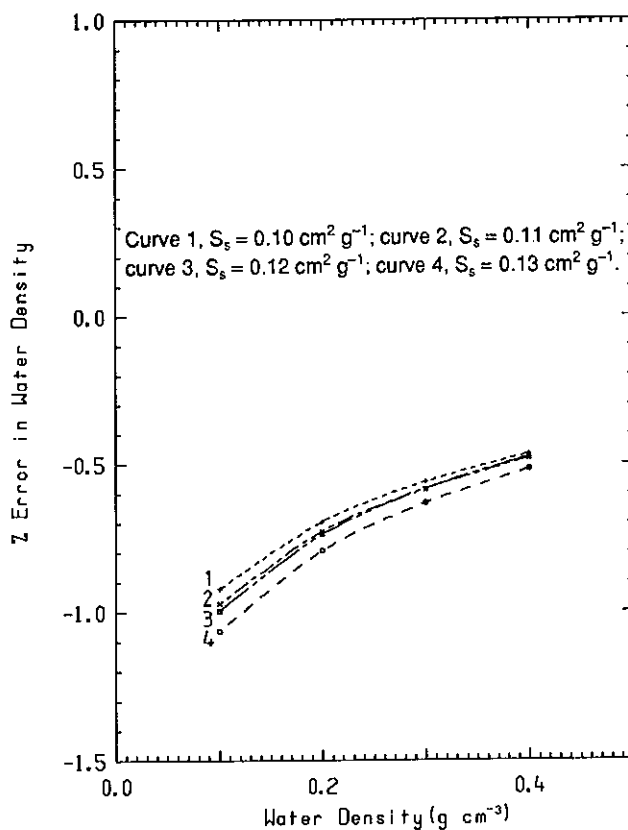


Figure 4c The percentage error in water density due to +1% error in the mass scattering coefficient; the effect of the mass scattering coefficient and the water density: $\rho = 1.33 \text{ g cm}^{-3}$, $S_a = 6.305 \times 10^{-3} \text{ cm}^2 \text{ g}^{-1}$.

APPENDIX A

The Polynomial Fits to Multigroup Calculations and Their Partial Differentials

1	$g = 2.2897 - 10.317 S_s$ $+ 37.114 S_s^2$	$\frac{\partial g}{\partial S_s} = - 10.317 + 74.228 S_s$
2	$h = - 1.0457 + 9.1333 S_s$ $- 48.066 S_s^2$	$\frac{\partial h}{\partial S_s} = 9.1333 - 96.132 S_s$
3	$j = 0.30622 - 3.5517 S_s$ $+ 17.5148 S_s^2$	$\frac{\partial j}{\partial S_s} = - 3.5517 + 35.030 S_s$
4	$m = - 0.17817 + 3.4872 S_s$ $- 15.2675 S_s^2$	$\frac{\partial m}{\partial S_s} = 3.4872 - 30.535 S_s$
5	$n = 0.43004 - 6.6776 S_s$ $+ 29.0533 S_s^2$	$\frac{\partial n}{\partial S_s} = - 6.6777 + 58.107 S_s$
6	$p = - 0.23389 + 3.5934 S_s$ $- 15.858 S_s^2$	$\frac{\partial p}{\partial S_s} = 3.5934 - 31.716 S_s$
7	$q = 0.039424 - 0.60089 S_s$ $+ 2.6996 S_s^2$	$\frac{\partial q}{\partial S_s} = - 0.60089 + 5.3992 S_s$
8	$r = 0.0068207 - 0.12652 S_s$ $+ 0.54766 S_s^2$	$\frac{\partial r}{\partial S_s} = - 0.12652 + 1.0953 S_s$
9	$s = - 0.012359 + 0.19601 S_s$ $- 0.83924 S_s^2$	$\frac{\partial s}{\partial S_s} = 0.19601 - 1.6785 S_s$
10	$t = 0.0039505 - 0.062828 S_s$ $+ 0.26984 S_s^2$	$\frac{\partial t}{\partial S_s} = - 0.062828 + 0.53968 S_s$
11	$d = g + hp + jp^2$	$\frac{\partial d}{\partial S_s} = \frac{\partial g}{\partial S_s} + \frac{\partial h}{\partial S_s} \rho + \frac{\partial j}{\partial S_s} \rho^2$

as $\frac{\partial \rho}{\partial S_s} = 0$

These partials and those to follow are all given in this table.

12	$e = m + np + pp^2 + qp^3$	$\frac{\partial e}{\partial S_s} = \frac{\partial m}{\partial S_s} + \frac{\partial n}{\partial S_s} \rho + \frac{\partial p}{\partial S_s} \rho^2 + \frac{\partial q}{\partial S_s} \rho^3$
13	$f = r + sp + tp^2$	$\frac{\partial f}{\partial S_s} = \frac{\partial r}{\partial S_s} + \frac{\partial s}{\partial S_s} \rho + \frac{\partial t}{\partial S_s} \rho^2$
14	$m = d + eS_a + fS_a^2$	$\frac{\partial m}{\partial S_s} = \frac{\partial d}{\partial S_s} + \frac{\partial e}{\partial S_s} S_a + \frac{\partial f}{\partial S_s} S_a^2$
15	$d = g + hp + jp^2$	$\frac{\partial d}{\partial \rho} = h + 2jp$
16	$e = m + np + pp^2 + qp^3$	$\frac{\partial e}{\partial \rho} = n + 2pp + 3qp^2$
17	$f = r + sp + tp^2$	$\frac{\partial f}{\partial \rho} = s + 2tp$
<hr/>		
18	$m = d + eS_a + fS_a^2$	$\frac{\partial m}{\partial \rho} = \frac{\partial d}{\partial \rho} + \frac{\partial e}{\partial \rho} S_a + \frac{\partial f}{\partial \rho} S_a^2$
19	$m = d + eS_a + fS_a^2$	$\frac{\partial m}{\partial S_a} = e + 2fS_a$
20	$c_{11} = 0.096324 - 1.5654 S_s$ $+ 40.597 S_s^3$	$\frac{\partial c_{11}}{\partial S_s} = -1.5654 + 121.79 S_s^2$
21	$c_{12} = 3811.1 (S_s - 0.11613)^2$ $+ 14.129$	$\frac{\partial c_{12}}{\partial S_s} = 7622.2 (S_s - 0.11613)$
22	$c_{13} = 18.017 + 181.53 S_s$ $- 913.42 S_s^2$	$\frac{\partial c_{13}}{\partial S_s} = 181.53 - 1826.8 S_s$
23	$c_{21} = 4.0980 - 22.812 S_s$ $+ 168.71 S_s^2$	$\frac{\partial c_{21}}{\partial S_s} = -22.812 + 337.42 S_s$
24	$c_{22} = 0.23097 - 30.776 S_s$ $+ 156.77 S_s^2$	$\frac{\partial c_{22}}{\partial S_s} = -30.776 + 313.54 S_s$
25	$c_{23} = -0.035523 + 1.2331 S_s$ $-6.4412 S_s^2$	$\frac{\partial c_{23}}{\partial S_s} = 1.2331 - 12.882 S_s$
26	$c_{31} = -10.621 + 191.62 S_s$ $- 697.68 S_s^2$	$\frac{\partial c_{31}}{\partial S_s} = 191.62 - 1395.4 S_s$
27	$c_{32} = 10.248 - 259.69 S_s$ $+ 912.36 S_s^2$	$\frac{\partial c_{32}}{\partial S_s} = -259.69 + 1824.7 S_s$

$$28 \quad c_{33} = -0.070231 + 0.40453 S_s - 0.79040 S_s^2 \quad \frac{\partial c_{33}}{\partial S_s} = 0.40453 - 1.5808 S_s$$

$$29 \quad c_{34} = -8.1071 + 218.12 S_s - 784.08 S_s^2 \quad \frac{\partial c_{34}}{\partial S_s} = 218.12 - 1568.2 S_s$$

$$30 \quad \phi_1 = c_{11}(S_a - c_{12})^2 + c_{13}$$

$$\frac{\partial \phi_1}{\partial S_s} = \frac{\partial \phi_1}{\partial c_{11}} \cdot \frac{\partial c_{11}}{\partial S_s} + \frac{\partial \phi_1}{\partial c_{12}} \cdot \frac{\partial c_{12}}{\partial S_s} + \frac{\partial \phi_1}{\partial c_{13}} \cdot \frac{\partial c_{13}}{\partial S_s}$$

$$= (S_a - c_{12})^2 [-1.5654 + 121.79 S_s^2] - 2c_{11}(S_a - c_{12})[7622.18(S_s - 0.116130)] + [181.53 - 1826.8 S_s]$$

The terms in square brackets are derived in lines 20, 21 and 22.

$$31 \quad \phi_2 = c_{21} + c_{22} S_a + c_{23} S_a^2$$

$$\frac{\partial \phi_2}{\partial S_s} = \frac{\partial c_{21}}{\partial S_s} + S_a \frac{\partial c_{22}}{\partial S_s} + S_a^2 \frac{\partial c_{23}}{\partial S_s}$$

$$= -22.812 + 337.42 S_s - 30.776 + 313.54 S_s + 1.2331 - 12.882 S_s$$

From lines 23, 24 and 25

$$32 \quad \phi_3 = \frac{c_{31}}{S_a} + c_{32} [\exp(c_{33} S_a)]$$

$$\frac{\partial \phi_3}{\partial S_s} = \left[\frac{1}{S_a} \right] (191.617 - 1395.356 S_a) + \exp(c_{33} S_a) (-259.693 + 1824.716 S_s) + c_{32} S_a [\exp(c_{33} S_a)] (0.40453 - 1.5808 S_s) + 218.12 - 1568.2 S_s$$

From lines 26, 27, 28 and 29

$$33 \quad \phi_0 = \phi_1 + \phi_2 \rho + \phi_3 \rho^2$$

$$\frac{\partial \phi_0}{\partial S_s} = \frac{\partial \phi_1}{\partial S_s} + \rho \frac{\partial \phi_2}{\partial S_s} + \rho^2 \frac{\partial \phi_3}{\partial S_s}$$

the partial differentials are given in lines 30, 31, 32

$$\begin{array}{ll} 34 & \phi_1 = c_{11}(S_a - c_{12})^2 + c_{13} \quad \frac{\partial \phi_1}{\partial S_a} = 2c_{11}(S_a - c_{12}) \\ 35 & \phi_2 = c_{21} + c_{22} S_a + c_{23} S_a^2 \quad \frac{\partial \phi_2}{\partial S_a} = c_{22} + 2c_{23} S_a \\ 36 & \phi_3 = \frac{c_{31}}{S_a} + c_{32} [\exp(c_{33} S_a)] \quad \frac{\partial \phi_3}{\partial S_a} = c_{32} c_{33} \exp(c_{33} S_a) - \frac{c_{31}}{S_a^2} \\ 37 & \phi_0 = \phi_1 + \phi_2 \rho + \phi_3 \rho^2 \quad \frac{\partial \phi_0}{\partial \rho} = \phi_2 + 2\rho \phi_3 \end{array}$$
